SSRG International Journal of Electrical and Electronics Engineering
ISSN: 2348-8379/ https://doi.org/10.14445/23488379/IJEEE-V12I8P107

Volume 12 Issue 8, 57-70, August 2025

Original Article

Application of ERPDC in LV Microgrids with Resistive Feeder Impedance

Devireddy Sathish[1], Pannala Krishna Murthy[2], Narri Yadaiah[3]

[1,3]*Department of Electrical and Electronics Engineering, Jawaharlal Nehru Technological University, Hyderabad, India.*
[2]*Department of Electrical and Electronics Engineering, Jayaprakash Narayan College of Engineering, Mahabubnagar, India.*

[1]*Corresponding Author : data.sathish@gmail.com*

Received: 05 June 2025 Revised: 07 July 2025 Accepted: 06 August 2025 Published: 30 August 2025

Abstract - *This paper explores the unique characteristics of both active and reactive power flow in Low-Voltage (LV) microgrids under different feeder impedance conditions during the parallel operation of distributed generators. It focuses on systems with mainly resistive feeder impedance, which pose challenges in accurate reactive power sharing and harmonic compensation. To address these challenges, the concept of an Enhanced Reactive Power Droop Controller (ERPDC) is applied as a control strategy. This method is developed to improve the distribution of reactive power and effectively reduce specific harmonic distortions, particularly the fifth and seventh harmonics that arise when non-linear loads are connected. The proposed approach is tested under various operating scenarios to evaluate its performance. Detailed simulations are carried out in the MATLAB Simulink environment, and results show that ERPDC offers better harmonic suppression and improved system stability when compared to conventional techniques.*

Keywords - *Droop control, Distributed generators, Power quality, Reactive power, Droop controller.*

1. Introduction

Advancements in the industrial sector and an increase in demand mean that power needs to be increased to meet the power requirements. In general, most of the power is produced from conventional energy sources. Over a period, the ratio of conventional sources may likely be depleted, which leads to more dependency on non-conventional energy sources. Recognizing their importance, diverse renewable energy sources are combined to form Distributed Generators (DGs), which are collectively termed as Microgrid [1]. Microgrids are particularly suitable for providing reliable energy solutions in remote and mountainous areas. The advantages of these sources are that they are pollution-free, eco-friendly, have a lower carbon footprint, and have less maintenance cost. A Microgrid operates in two modes based on system requirements: grid-connected mode, where it synchronizes with the main utility grid, and islanded mode, where it functions autonomously without external power support [2]. Currently, DGs are interfaced to the primary power grid using converter technology. The rapid advancement in power electronic technologies has enabled the deployment of multilevel inverters in modern power systems, allowing engineers to address high power demands more efficiently and cost-effectively. These inverters enhance output voltage quality, reduce total harmonic distortion, and minimize stress on power switches. However, when multiple inverters are connected in parallel, particularly in Distributed Generation (DG) based microgrids, one of the key technical challenges is achieving accurate and stable load sharing among the units. This becomes critical because improper load distribution can lead to circulating currents, unequal power contribution, and potential overloading of individual inverters. The coordination of these inverters requires sophisticated control strategies that ensure synchronized operation, maintain voltage and frequency stability, and preserve system reliability even under varying load or generation conditions. The increasing use of advanced power electronic devices helped power system engineers meet the high power demand by using multilevel inverters at a low cost. The primary challenge with parallel-operated inverters is the distribution of load among the DGs.

In microgrid operations, the conventional droop control method is widely adopted due to its key advantages, such as decentralized operation without the need for external communication and its ability to enable effective power sharing among Distributed Generation (DG) units, particularly under linear load conditions. Droop control is effective for DG units under linear load conditions, but it requires all inverters to have uniform per-unit impedance and identical RMS voltage references. Meeting these conditions is difficult in practice due to parameter mismatches and dynamic load variations. Communication-based coordination strategies are sometimes employed to address these limitations and improve system performance, especially in the presence of non-linear

or unbalanced loads. These external communication techniques support enhanced functions such as precise load sharing and restoration of system voltage and frequency.

The authors in [3] proposed a small signal injection technique to improve harmonic current sharing. This was achieved by combining voltage droop for non-linear load distribution and precise reactive power allocation. The conventional droop controller was originally designed for systems with resistive feeder impedance, enabling effective power distribution to both the loads in islanded Microgrid operations [4]. Reactive power sharing becomes unreliable at certain frequencies, which highlights the need for a more effective control strategy to ensure power is shared according to the inverter's rated capacity. To overcome this limitation, an improved droop controller was introduced in [5-7] by adding an integral component to the conventional droop control design for better performance. These controllers are capable of compensating for voltage drops by dynamically adjusting the droop coefficients. Persistent challenges at the Point of Common Coupling (PCC) include imbalances in power distribution, instability in voltage and frequency levels, and the presence of waveform distortions due to harmonics.

To resolve these problems, a secondary control method is employed to regulate voltage and frequency back to their reference levels. The authors proposed [8-11] a novel control technique known as the secondary control system, which contributes to improved voltage and frequency regulation; however, it may experience challenges such as delayed response time and stability concerns under certain conditions. Effective methods have been developed for managing and distributing linear loads in Microgrids [12, 13]. However, when non-linear loads are connected, they generate harmonic currents that flow through the inverter’s output impedance, causing voltage distortion and drops. Power quality can be improved by mitigating these harmonic voltage distortions or by efficiently sharing harmonic currents at PCC [13].

Harmonic current distribution methods were mainly classified into two groups based on the methods that rely on communication. Communication-based methods enable harmonic current sharing by transmitting PCC voltage data to a central controller via a communication link. Decentralized methods [13] depend on local measurements and operate without the need for any communication infrastructure. These methods for harmonic power distribution can be further categorized into virtual resistance, impedance, and conductance approaches. The virtual resistance method [14] was the initial technique introduced for harmonic power distribution, where the inverter's output impedance is modified by incorporating virtual harmonic resistance. While the positive harmonic resistance technique increases the effective line impedance, it reduces voltage quality across the PCC. The authors introduced the negative virtual harmonic impedance concept to address these issues. This method facilitates effective harmonic current distribution by maintaining voltage quality. In decentralized approaches, the droop controller produces a reference voltage signal for each primary harmonic voltage component. While the proposed approach [15] enhances the voltage profile at the terminals of Distributed Generation (DG) units, its effectiveness in distributing harmonic currents is limited, as the reference voltage produced does not depend on the output current.

In islanded microgrid systems, centralized harmonic current control methods require constant data exchange between inverters through communication networks. This heavy reliance on communication makes the system prone to issues such as latency, data loss, or link failure, which can disrupt harmonic compensation and compromise the reliability and stability of the microgrid. In contrast, decentralized control methods do not rely on communication networks but often face challenges in evenly sharing harmonic currents. This is mainly due to the absence of complete system-wide information, leading to inaccurate compensation and reduced effectiveness in mitigating harmonics across the microgrid.

Inverters are considered as voltage sources with inductive impedance that may cause distortion under nonlinear loading and harmonic conditions. To improve current distribution and maintain voltage stability, a virtual resistance is included in the control strategy. To address this issue, a robust droop controller has been introduced by the authors in [16, 17] to manage the inverters' inherent impedance. This method uses a feed-forward harmonic current loop to dynamically tune the inverter's impedance, allowing real-time adjustment of harmonic impedance according to the harmonic power output.

After analysing potential challenges in numerical computations, parameter variations, and equipment inconsistencies, this article presents a typical approach to enhance the reliability and efficiency of parallel-operated inverters. By focusing on two major conditions that ensure load sharing is proportional to their ratings, the authors propose a robust droop control technique that guarantees precise power distribution according to the ratings of the inverters. This controller regulates output load voltage and effectively mitigates the voltage drop effect, paving the way for more efficient and reliable power systems [18]. Robust droop controllers have limitations such as the need for complex tuning to maintain stability under varying load conditions and slower dynamic responses that can reduce the system’s ability to quickly adapt to sudden changes.

Based on the limitations identified above, the controllers are not suitable for LV Microgrids with resistive feeder impedance. To overcome the limitations of all the methods, an improved form of the reactive power droop controller, referred to as the Enhanced Reactive Power Droop Controller (ERPDC), is utilized. This approach improves overall system

performance, enables effective sharing of harmonic reactive power, and ensures equal circulation of harmonic currents among the DGs. The organization of the paper in Section 2 provides an overview of the Microgrid system along with its mathematical modelling. Section 3 discusses the droop control strategy, including modelling the conventional droop control and its modified version under various operating conditions. Section 4 describes the Concept of ERPDC for LV Microgrids with Resistive feeder impedance, Algorithm of ERPDC and its applications. Section 5 presents the results along with detailed analysis, while Section 6 concludes with the final observations and potential directions for future research.

2. Overview of Microgrid System

A microgrid consists of a combination of individual sources, which are named as DGs. LV Microgrids are suitable for remote areas, communities, or individual buildings, providing a resilient and sustainable energy solution. Figure 1 illustrates a schematic Representation of a Microgrid system, where all Distributed Generators (DGs), inverters, filters, and feeder impedances are interconnected at a single point known as the PCC. The PCC is essential for maintaining stable and uniform voltage levels across all DG units. A schematic representation of a Microgrid system is shown in Figure 1, supplying power to both linear and non-linear loads.

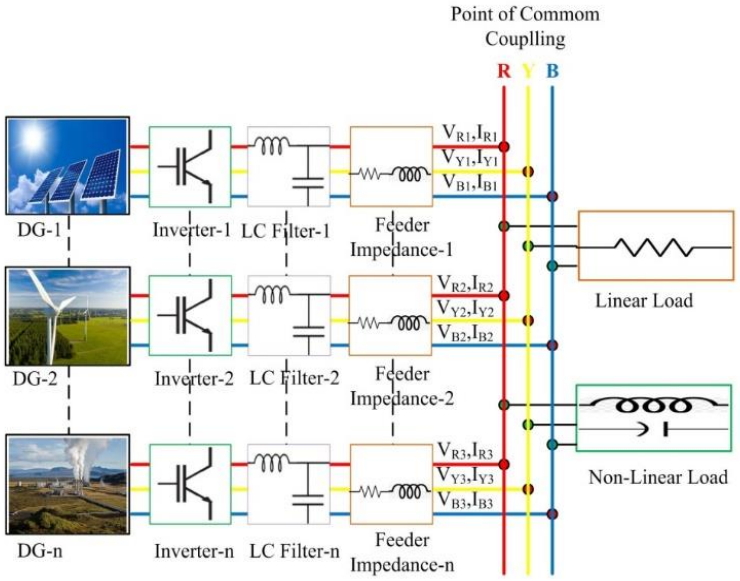

Fig. 1 A schematic representation of a microgrid system

Electricity is produced locally using multiple Distributed Generation (DG) units, including solar panels, wind turbines, and hydro sources. These DG units typically generate Direct Current (DC), which must be converted to Alternating Current (AC) to comply with the grid standard. Each DG is connected to an inverter that uses semiconductor components to perform this DC-to-AC conversion. Once converted, the AC power flows through LC filters-made up of inductors and capacitors-that eliminate high-frequency harmonics and enhance the quality of the electrical waveform. The filtered AC outputs are then combined at a common point called the PCC, forming a unified three-phase system represented by R (Red), Y (Yellow), and B (Blue) lines. At this PCC, different types of loads are connected to consume the generated power. The linear load, represented by a resistor, consumes power in a predictable manner without introducing harmonic distortion. In contrast, the non-linear load, which includes components like inductors and switches, draws current in a non-sinusoidal fashion and contributes to harmonic pollution. Overall, this system demonstrates how multiple distributed energy resources can be integrated and filtered before supplying a combination of linear and non-linear loads in a clean and stable manner.

The authors in [3-6] concentrated on the islanded mode of operation in Microgrid, which presents unique challenges like voltage and frequency instability due to power imbalance and low system inertia. Unequal sharing of reactive power and harmonic currents among DGs leads to poor power quality and overloading. Unlike a grid-connected system, an autonomous Microgrid must generate its reference voltage and frequency according to the load demand. Currently, DGs are interfaced to the primary power grid using converter technology. The increasing use of advanced power electronic devices helped power system engineers meet the high power demand by using multilevel inverters at a low cost. The primary challenge with parallel-operated inverters is the distribution of load among the DGs.

2.1. Modelling of Microgrid System

The development of high-performance systems necessitates the creation of accurate mathematical models for

loads, Distributed Generators (DGs), and LC filters, as these models form the foundation for optimizing system efficiency and effectiveness. The mathematical model of the Microgrid, illustrated in Figure 2, is derived as a schematic representation, with its corresponding phasor diagram shown in Figure 3, as referenced in [19].

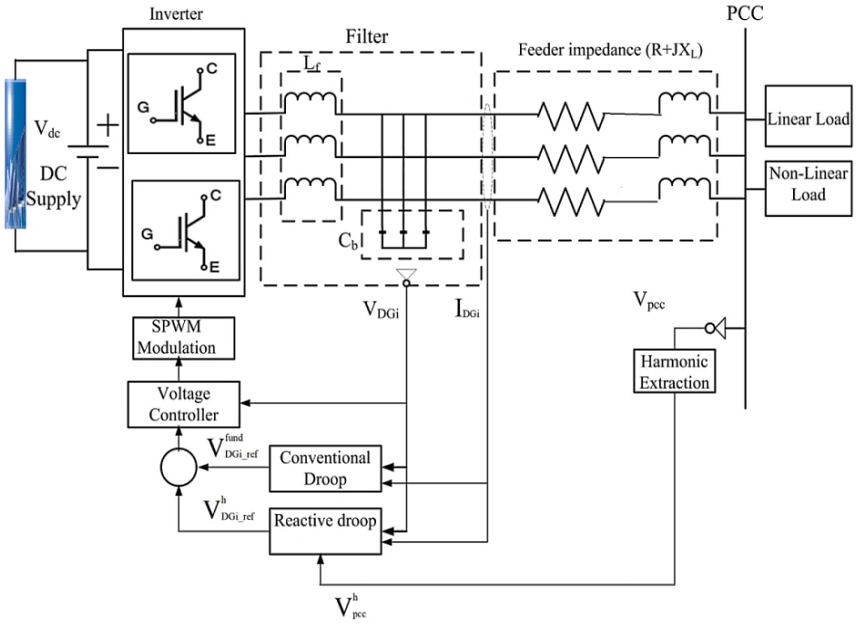

Fig. 2 Detailed schematic diagram of a DG connected to a microgrid

Figure 2 shows the fundamental active power and reactive power drawn by the load.

$$P = \sqrt{3}\ VI\ \ Cos\theta\ \ , Q = \sqrt{3}\ VI\ Sin\theta \qquad (1)$$

Where, $V = V_{DGi}$ & $I = I_{DGi}$ are line-line values, cosϴ is the power factor of the system.

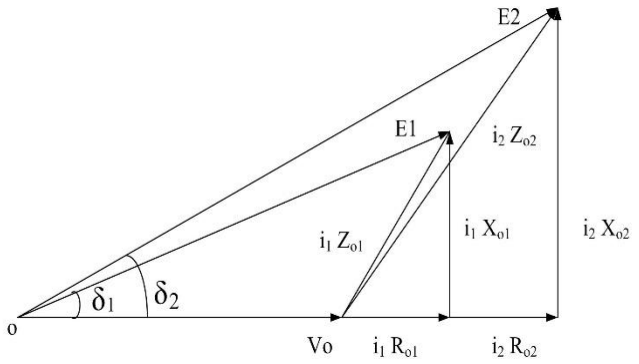

Fig. 3 Phasor diagram of two parallel inverters

In LC filter design, it is essential to define the maximum permissible AC current ripple. In this case, the inverter-side inductance is chosen as 5% of the rated phase current. With a fixed DC link voltage and switching frequency, the converter-side inductance L_f is determined based on the specified ripple current ΔI_{pmax}. To suppress high-frequency components before grid connection, the filter provides low shunt impedance at high frequencies, ensuring effective attenuation. To select the filter capacitance, a maximum power factor variation of 5% at the grid side is considered. Based on this criterion, the necessary values of inductance and capacitance are calculated using the following relation:

$$L_f = \frac{V_{DC}}{16\ f_s\ \Delta I_{pmax}},\ C_b = \frac{1}{W_g Z_b} \qquad (2)$$

Where Lf is the filter inductance, fs is the system frequency, I_{pmax} is the maximum peak current, C_b is the base filter capacitance, W_g is the base system frequency, and Z_b is the base impedance of the system.

The DC bus voltage (V_{DC}) of the filter is determined by the line voltage at the PCC. For a three-phase Voltage Source Inverter (VSC), the required DC bus voltage is calculated using the following equation

$$.V_{DC} = \frac{2\sqrt{2}V}{\sqrt{3}m} \qquad (3)$$

Where V is the line-to-line voltage, m is the modulation index of the inverter. The VA rating of the filter 'S' can be estimated using the equation.

$$S = 3V_{ph}I_{ph} \qquad (4)$$

V_{ph} is the phase voltage of the system, and I_{ph} is the current phase of the system.

3. Droop Control Technique

The droop control method is used in islanded microgrids, where generators adjust their output based on frequency and voltage changes, ensuring active and reactive power balance. It allows for autonomous power sharing between distributed energy resources without the need for communication. This technique helps maintain stability in the microgrid while allowing for flexibility and scalability.

3.1. Modeling of a Conventional Droop Controller

Conventional droop controllers are widely used techniques to control active and reactive power sharing. Mainly used for low-voltage Microgrid applications. Thereby, the modelling of a conventional droop controller plays a main role in the effective operation of the system. For accurate modelling of conventional droop controllers, it is necessary to estimate power equations and power delivered through impedance [15]. Therefore, calculations of power equations and power delivered through impedance are obtained from Figure 4 of parallel-connected inverters. The reference voltages (V_{DG1_ref1}, V_{DG2_ref2}) for the two inverters are given as follows.

$$V_{DG1\_ref1} = \sqrt{2}E_1\sin(\omega_1 t + \delta_1) \quad (5)$$

$$V_{DGi\_ref2} = \sqrt{2}E_2\sin(\omega_2 t + \delta_2) \quad (6)$$

In this context, E_1 and E_2 represent the RMS voltage reference values for the inverters. The power capacities of the inverters are given as follows:

$$S_1 = EI_1^* \text{and } S_2 = EI_2^* \quad (7)$$

The two inverters will have a common voltage, i.e.,

$$V_1 = V_{DG1\_ref1} - R_{01}i_1 = V_{DG1\_ref2} - R_{02}i_2 \quad (8)$$

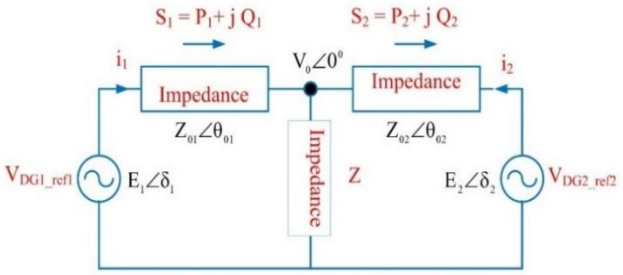

Fig. 4 Two inverters (DGs) are connected in parallel

Similarly, power supplied to a Voltage Source via impedance is represented in Figure 5. From Figure 5, it can be observed that the input source voltage *(V_r)* will deliver power to the output voltage (*Vo*) via line impedance (*Z_0 ∠θ*). By applying Kirchhoff's Voltage Law (KVL) to the loop, the resulting current equation can be calculated as follows.

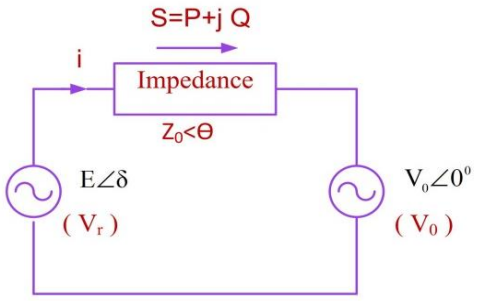

Fig. 5 Power is supplied to a voltage source via impedance

$$i = \frac{E\angle\delta - V_0\angle 0^0}{Z_0\angle\theta} \quad (9)$$

$$i = \frac{E\cos\delta - V_0 + j\,E\sin\delta}{Z_0\angle\theta} \quad (10)$$

Apparent power of the system $S = V_0\, i^*$ (11)

By substituting Equations (9), and (10) in equation (11), the active and the reactive power can be derived. i.e.,

$$P = \left(\frac{E\,V_0}{Z_0}\cos\delta - \frac{V_0^2}{Z_0}\right)\cos\theta + \frac{E\,V_0}{Z_0}\sin\delta\,\sin\theta \quad (12)$$

$$Q = \left(\frac{E\,V_0}{Z_0}\cos\delta - \frac{V_0^2}{Z_0}\right)\sin\theta - \frac{E\,V_0}{Z_0}\sin\delta\,\cos\theta \quad (13)$$

This context δdenotes the phase difference between the source voltage (E) and the terminal voltage (V_o). The traditional droop control makes it difficult to precisely calculate the reactive power at a particular harmonic frequency. Consequently, it necessitates modifying the controller to meet the specific needs of the application. Figure 5. It shows the control diagram for this system. To ensure the inverters share the load according to their power ratings, their droop coefficients should be set inversely proportional to those ratings.

$$n_1 S_1^* = n_2 S_2^* \quad (14)$$

$$m_1 S_1^* = m_2 S_2^* \quad (15)$$

It is evident that n_i and m_i also fulfil the following condition:

$$\frac{n_1}{m_1} = \frac{n_2}{m_2} \quad (16)$$

The development of high-performance systems necessitates the creation of accurate mathematical models for loads, Distributed Generators (DGs), and LC filters, as these models form the foundation for optimizing system efficiency and effectiveness.

3.2. Modified Conventional Droop Controller

Modified Droop Controller is a control strategy used in inverter-based distributed generation systems to regulate voltage and frequency based on power output [17]. As shown in Figure 6, the process begins with the measurement of the output voltage V0 and current i, based on which the controller computes the active and reactive power.

$$P_i=V_{0.}\, i.\, Cos\theta \quad (17)$$

$$Q_i=V_{0.}\, i.\, Sin\theta \quad (18)$$

These real-time power values reflect the system's interaction with its load or the grid and form the basis for the droop adjustments. The droop mechanism modifies frequency and voltage references in proportion to power levels using droop coefficients m_i and n_i. The equations used are:

$$\Delta f = -m_i.P_i \ , \Delta E = -n_i.Q_i \quad (19)$$

These deviations are then added to nominal values to form updated references:

$$\omega^* = \omega_0 + \Delta f,\ E^* = E_0 + \Delta E \quad (20)$$

This helps the system mimic the behavior of synchronous generators, improving load sharing in parallel operation. Next, the controller integrates the frequency reference to generate the phase angle needed for inverter operation:

$$\theta_i = \int \omega^* + dt = \omega_i t + g_i \quad (21)$$

Similarly, the voltage reference E^* is integrated to form the internal voltage signal E_i, which determines the output voltage magnitude. These signals serve as critical inputs to the inverter's Voltage Controller. A voltage correction loop has been added to enhance voltage accuracy and dynamic performance. It compares the desired voltage reference E^* with the actual measured RMS voltage V_{RMS}, producing an error:

$$\Delta V = E^* - V_{RMS} \quad (22)$$

This error is scaled by a proportional gain Ke to generate a correction term:

$$\text{Correction}=Ke\cdot (E^* - V_{RMS}) \quad (23)$$

This correction is fed back into the voltage control path and added to E_i, ensuring better voltage regulation, especially during transients. Finally, the refined signals $E_i$and $\theta_i$are provided to the Voltage Controller, which produces control outputs for the inverter to maintain the desired voltage waveform. An optional external voltage reference $V_{ri\ can}$ be used to coordinate the system with supervisory controls or grid operations. Overall, the Modified Droop Controller ensures stable and adaptive operation under varying load and grid conditions, combining traditional droop principles with feedback correction for enhanced performance.

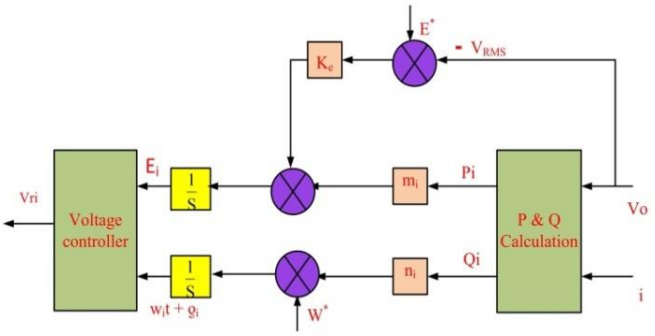

Fig. 6 Block diagram of the modified droop controller

4. Concept of ERPDC for LV Microgrids with Resistive Feeder Impedance

The conventional and modified droop controllers can be used only for linear loads and cannot be used for non-linear loads. The authors used the concept of ERPDC to apply LV Microgrids. The primary goal of this approach is to manage power quality effectively in the presence of nonlinear loads and resistive feeder impedance. It focuses on achieving balanced reactive power distribution among DGs, reducing voltage harmonic distortion at the PCC, and ensuring stable system operation. By continuously tuning control parameters according to real-time system conditions, the controller improves the efficiency and robustness of the distributed generation system under different loading scenarios. The ERPDC is developed based on the fundamental principles of the traditional droop control method, as shown in Figure 7.

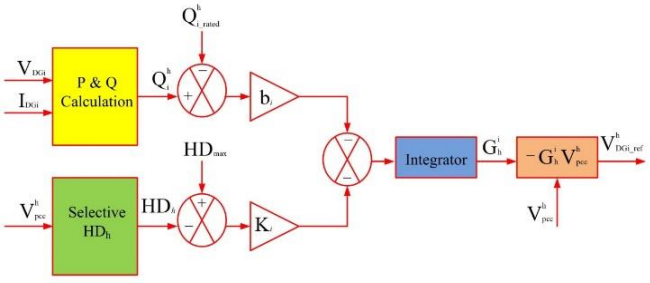

Fig. 7 Concept of ERPDC method

From Figure 7, the positive gain ($\boldsymbol{G_i^h}$) is defined in terms of the measured harmonic reactive power ($\boldsymbol{Q_i^h}$) and rated harmonic reactive power ($\boldsymbol{Q}^{\boldsymbol{h}}_{\text{i\_rated}}$). The gain factor in a harmonic droop controller plays a critical role in ensuring accurate harmonic compensation and power-sharing among DG units. In addition, gain factors will also help in managing accurate harmonic power sharing among multiple DG units. By tuning the gain factor within the droop control strategy, the

harmonic load can be proportionally distributed according to each unit's capacity. Improper tuning may lead to uneven harmonic current sharing, causing voltage distortion or overloading of certain DG units. Further, insufficient gain may result in poor harmonic attenuation, while an overly aggressive gain can lead to system instability or overcompensation effects.

For all the DGs, the Harmonic droop coefficients α_i is inversely proportional to the reactive power from (14) and (15) Equations are defined as:

$$\alpha_1 \ Q^h_{1\_rated} = \alpha_2 \ Q^h_{2\_rated} = \alpha_3 \ Q^h_{3\_rated} \ldots\ldots\ldots = \alpha_n \ Q^h_{n\_rated} \quad (24)$$

To achieve proportional sharing of harmonic reactive power among DG units despite differences in line impedance, the proposed harmonic droop method integrates a common control component. As shown in Figure 2, the selected harmonic distortion (HD_h) is compared with a predefined reference value to minimize the resulting error to zero. Since the common control component is uniformly applied to all DG units, it ensures consistent harmonic regulation, leading to the formulation of the following equation.

$$\alpha_1 \ (Q^h_{1\_rated} - Q^h_1) = \alpha_2 \ (Q^h_{2\_rated} - Q^h_2) = \alpha_3 \ (Q^h_{3\_rated} - Q^h_3) \ldots\ldots\ldots\ldots = \alpha_n \ (Q^h_{n\_rated} - Q^h_n) \quad (25)$$

Consistent with Equation (24), the harmonic reactive power is proportionally allocated and can be expressed as

$$\alpha_1 \ Q^h_1 = \alpha_2 \ Q^h_2 = \alpha_3 \ Q^h_3 \ldots\ldots\ldots\ldots = \alpha_n \ Q^h_n \quad (26)$$

The harmonic reactive power drawn by each DG corresponds to its specific frequency. It can be given in Equation (32)

$$Q_i^h = 3 \ V^{fund}_{DGi} \ I^h_{DGi} \quad (27)$$

$V^{fund}_{DG\_i}$= The fundamental RMS voltage at the output of DG_i.

$I^h_{DG\_i}$= The h-harmonic current passing through the line impedance of DG_i.

From Equations (14) and (15), the harmonic droop coefficients are determined as given below.

$$\alpha_i = \frac{\alpha_0}{Q^h_{i\_rated}} \quad (28)$$

The gain α_0 is the key parameter, and this can be effectively tuned to get accurate harmonic power sharing, which makes the system stability good at all times. For all the DG units, the gain K_h is defined, and the equation is

$$K_h = \frac{\alpha_o}{HDmax} \quad (29)$$

To properly configure the suggested reactive power droop controller, it is essential to adjust the gain α_0 based on the maximum harmonic distortion HD_{max}. This controller adapts the gain dynamically in response to the particular harmonic frequency. Consequently, this controller generates a harmonic reference output voltage for each Distributed Generator. The harmonic distortion at the PCC can be expressed as:

$$HD_h = \frac{V^h_{pcc}}{V^{fund}_{pcc}} \quad (30)$$

When a harmonic reference voltage is applied to the input of the DG's inner controller, it is crucial to avoid saturation. To achieve this, the integrator in the proposed harmonic droop control must be constrained within the inverter's saturation limits, depending on the modulation method used. For Sinusoidal PWM, the saturation threshold is defined as:

$$V_{DGi\_ref} = \sqrt{\frac{3}{2}} \ X \ \frac{V_{DC}}{2} \quad (31)$$

Once the harmonic reference voltage is integrated into the inner controller of the Distributed Generator, the reference RMS voltage, DG_i_ref, can be expressed as:

$$V_{DGi\_ref} = \sqrt{(V^{fund}_{DG\_i\_ref})^2 + (V^h_{DG\_i\_ref})^2} \quad (32)$$

The reference voltage for the h-harmonic can be expressed as:

$$V^h_{DGi_{ref}} = -G^h_i V^h_{pcc} \quad (33)$$

$$V^h_{DGiref(max)} = -G^h_i HD_{max} V^{fund}_{pcc} \quad (34)$$

From Equations (32),(33), and (34), the conductance (G_i^h) value can be given as

$$0 \le G^h_i \le \frac{\sqrt{\frac{3}{2}\left(\frac{V_{DC}}{2}\right)^2 - (V^{fund}_{DGi})^2}}{HD_{max} V^{fund}_{DGi}} \quad (35)$$

4.1. Implementation of EPRDC

1. Measure Local Quantities:
   - Measure voltage (V), frequency (f), active power (P), and reactive power (Q) at each DG.

2. Calculate Droop References:
   - Calculate frequency reference f_{ref} using P-f droop: f_{ref}= f_{rated}- m*P
   - Calculate voltage reference V_{ref}using Q-v droop: $V_{DG\_i\_ref}$= V_{rated}- n*Q

Where m_i: P-f droop coefficient, n_i: Q-v droop coefficient, f_{rated}: Rated frequency, V_{rated}: Nominal voltage, P_{rated} Nominal active power, Q_{rated}: Nominal reactive power, ΔV: Acceptable voltage deviation, Δf: Acceptable frequency deviation.

3. Virtual Impedance Control:
   - Implement virtual impedance Z_{var} to enhance stability and power sharing.

4. Power Sharing and Regulation:
   - Adjust droop coefficients (m_i, n_i) to achieve desired power sharing among DGs.
   - Regulate voltage and frequency within acceptable limits.

5. Stability Enhancement:
   - Implement additional control loops to enhance stability and damping.

6. Output Control Signals:
   - Generate control signals for each DG to adjust their output voltage and frequency.

Further, the flowchart of the ERPDC is clearly presented in Figure 8.

4.2. Application of ERPDC in LV Microgrids with Resistive Feeder Impedance

The concept of ERPDC proves to be highly beneficial across a range of practical applications in low-voltage Microgrids, especially those with resistive feeder impedances. In residential Microgrids featuring significant solar PV integration, this control method enables inverters to share the responsibility of mitigating harmonic distortion independently, thereby enhancing overall voltage quality without relying on communication systems.

For Microgrids in rural or remote locations, the controller supports stable operation despite varying load demands and generation levels, while also facilitating straightforward integration of additional energy resources. Commercial facilities housing sensitive equipment, such as hospitals and data centers, benefit from reducing voltage distortion, which is critical to maintaining the proper functioning of essential devices; harmonic droop control plays a key role in ensuring power purity in these environments.

Likewise, electric vehicle charging stations use this approach to suppress harmonics generated by fast chargers, contributing to the stability of the local grid and preventing undue wear on electrical components. Lastly, in industrial settings where nonlinear loads like variable frequency drives and welding machines are prevalent, this strategy helps avoid the installation of costly harmonic filters, delivering consistent and clean power to support efficient and reliable operations.

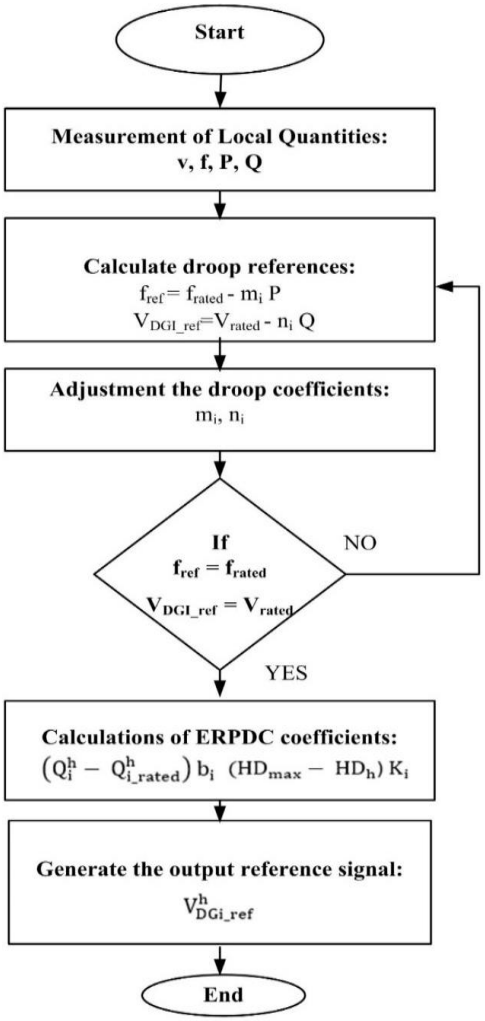

Fig. 8 Flowchart of the ERPDC

5. Results

The mathematical model was developed for the system and integrated into the complete Microgrid system of power rating S=2.6425 KVA. The developed MATLAB was used to assess the effectiveness of the proposed method, and we considered the system parameters given in Table 1.

Table 1. Ratings of the modeled system

S.No	Parameters(s)	Values
1	Fundamental Active power (P)	1800 W
2	Fundamental Reactive power (Q)	1100 Var
3	Total Apparent power (S)	2114.789 VA
4	Input DC voltage	220 V
5	Power Factor(cosθ)	0.8533
6	Filter Inductance (L_f)	5 mH
7	Filter Capacitance (C_f)	30 μF
8	Fundamental Line current (I_1)	9.44 + j 5.7708 A
9	Fifth Harmonic Line Current Line	6 - j2 A

	current (I_5)	
10	Seventh Harmonic Line Current Line current (I_7)	-5 + j10 A
11	Total Harmonic line current (I_h)	10.44+j 3.7708 A
While designing the inverter, the rating is 1.25 times the apparent power. S= 2.6425 KVA, P=2.486 KW, Q=900VAR. (Approximate Design parameters)		

Models were tested by considering the Conventional droop controller and the EDPDC method under nonlinear load conditions. In addition, a conventional droop controller is also tested under linear load conditions to test the performance of the developed models.

5.1. Implementation of the Conventional Droop Controller with Linear Load

When two DGs are connected to the PCC and supply a linear load using a conventional droop controller, the currents and voltages at the PCC remain sinusoidal, and each DG exhibits distinct current and voltage characteristics. Linear loads draw current proportional to the applied voltage without introducing harmonic distortions. Thereby, it allows the DGs to maintain clean, undistorted waveforms. The droop controller facilitates effective power-sharing between the DGs, reduces Total Harmonic Distortion (THD), and enhances overall system reliability. This setup ensures a stable and high-quality power supply, leading to efficient operation of connected devices and reduced energy losses. The developed system is simulated for 5 seconds. The obtained waveforms in this case are presented in Figure 9. The waveforms represent the PCC current, the current at DG1, and the current at DG2, respectively. The analysis of this waveform can be divided into three distinct phases, namely the transient Phase (0 – 1.5 sec), transition Phase (1.5 – 2.5 sec), and steady-state Phase (after 2.5 sec).

Figure 9(a) represents a harmonic current at the PCC in a three-phase system. The plot shows the variation of three-phase currents over time in amperes (A) along the y-axis, while the x-axis represents time in seconds. Initially, 0 - 1.5 sec, the system starts with a transient behavior where the current has fluctuations. A label indicates that "Conventional droop is initiated," which suggests that a droop control mechanism is applied to regulate power sharing. During the transition phase (i.e., 1.5 - 2.5 sec), the current shows large oscillations, likely due to the system responding to a change in load or control strategy. In Steady State, after 2.5 sec, the current waveform becomes more uniform and periodic. This indicates that the system has settled into a steady-state operation. A zoomed portion highlights the three-phase sinusoidal nature of the current in this stable state. Figures 9 (b) and (c) represent the harmonic current at DG_1 and DG_2 in a three-phase power system. Initially, in the transient Phase from 0 to 1.5 sec, the waveform initially exhibits high-frequency oscillations, suggesting a transient response when the system starts. The label "Conventional Droop is initiated" indicates that a droop control strategy is applied to regulate power sharing among distributed generating sources. The amplitude of current oscillations is significant, implying that the system is adjusting to the new operating conditions. In the Transition Phase from 1.5 - 2.5 sec, the waveform gradually stabilizes, with decreasing oscillation amplitude. The two labels in Figure 9 (b) and (c) mark the transition period where the system moves toward a steady state. In steady-state operation, after 2.5 sec, the current waveform achieves a periodic and balanced three-phase pattern. A zoomed-in section highlights the steady-state harmonic behavior of the three-phase current.

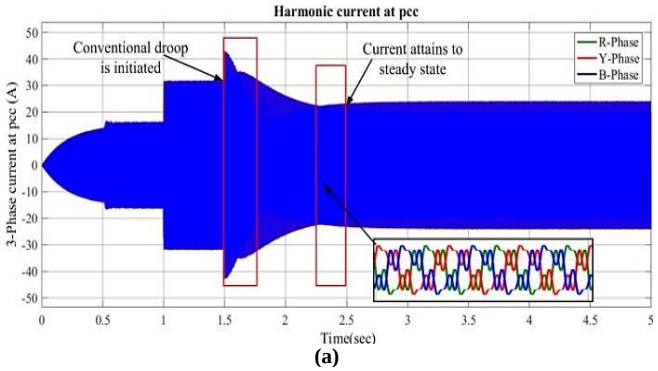

(a)

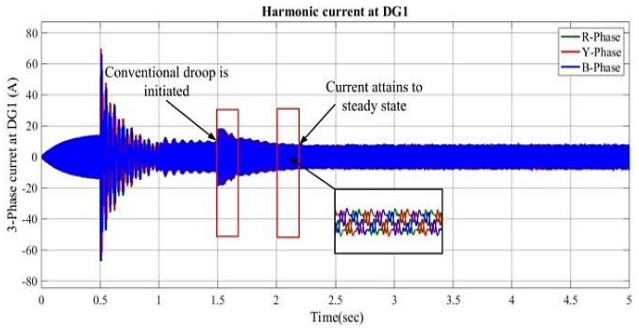

(b)

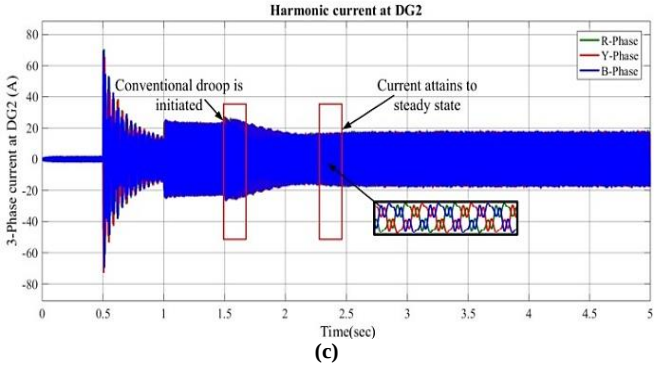

(c)

Fig. 9 (a) Harmonic current at PCC, (b) Harmonic current at DG1, and (c) Harmonic current at DG2.

Similarly, the developed system is simulated for 5 seconds and voltages of DG_1, DG_2 and PCC are captured and

presented in Figure 10. Figure 10(a) represents the voltage at the PCC in a three-phase system. The plot shows the variation of three-phase voltage over time in amperes (A) along the y-axis, while the x-axis represents time in seconds. Initially, 0 - 1.5 sec, the system starts with a transient behavior where the voltage has fluctuations.

A label indicates that "Conventional droop is initiated," which tells that a droop control mechanism is applied to regulate power sharing. In the Transition Phase from 1.5 - 2.5 sec, the voltage is trying to stabilize. The two labels highlight regions where the system undergoes instability before reaching steady-state behavior. In Steady-State, after 2.5 sec, the voltage waveform becomes more uniform and periodic, indicating that the system has settled into a steady-state operation. A zoomed-in section highlights the three-phase sinusoidal nature of the voltage in this stable state.

Further, Figures 10 (b) and (c) represent the voltage at DG_1 and DG_2 in a three-phase power system. Initially, in the transient Phase from 0 to 1.5 sec, the waveform exhibits high-frequency oscillations. The label "Conventional Droop is Initiated" indicates that a droop control strategy is applied to regulate power sharing among distributed generating sources.

The amplitude of voltage oscillations is significant, implying that the system is adjusting to the new operating conditions. In the transition Phase from 1.5 - 2.5 sec, the waveform gradually stabilizes, with decreasing oscillation amplitude. The two labels mark the transition period where the system moves toward a steady state. In steady-state operation, after 2.5 sec, the voltage waveform achieves a periodic and balanced three-phase pattern. A zoomed-in section highlights the steady-state harmonic behavior of the three-phase voltage.

It can be observed that the conventional droop control is initiated at 2 seconds**,** and the system gradually stabilizes, reaching a steady-state condition around 3.5 seconds, as represented in Figures 11(a) and (b). This balanced power distribution ensures stable system operation. The corresponding waveforms, shown in Figures 11(a) and 11(b), illustrate the effectiveness of this power-sharing mechanism and the system's transition toward steady-state operation.

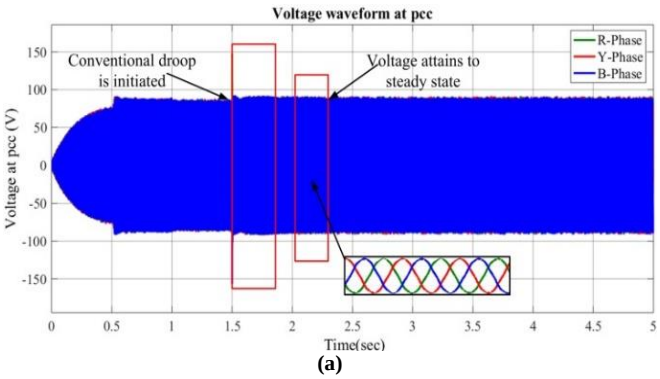

(a)

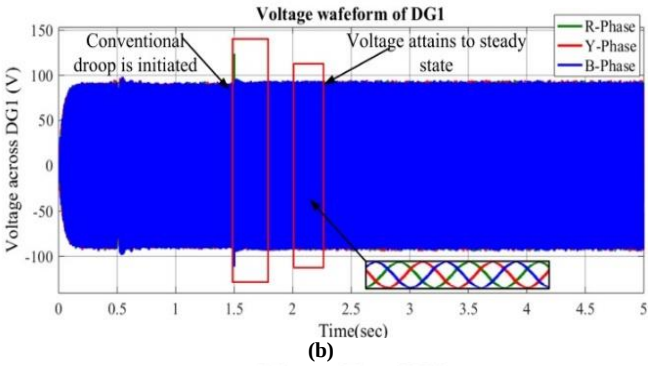

(b)

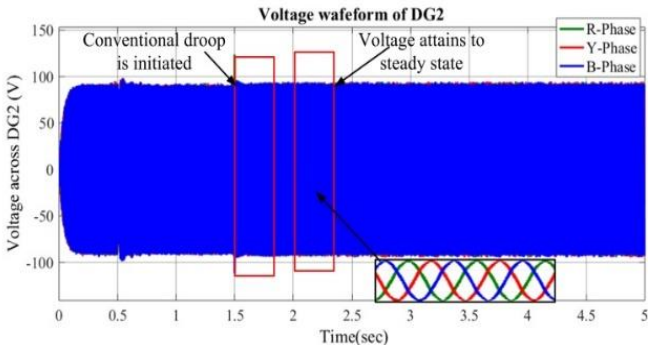

(c)

Fig. 10 (a) Voltage at PCC, (b) Voltage at DG1, and (c) Voltage at DG2.

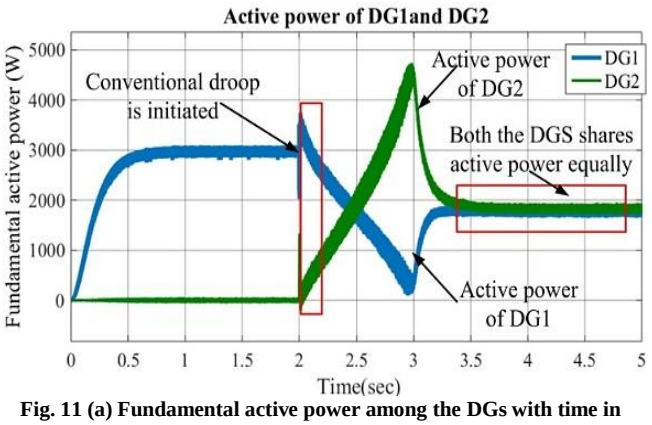

Fig. 11 (a) Fundamental active power among the DGs with time in seconds

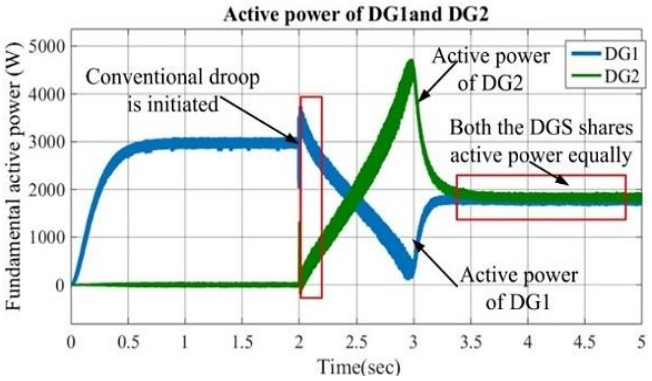

Fig. 11 (b) Fundamental Reactive power among the DGs with time in seconds

5.2. Implementation of the Conventional Droop Controller with Non-Linear Load

When nonlinear loads are connected to a system utilizing a modified droop control strategy, it has been observed that the reactive power at specific harmonic frequencies, such as the 5th and 7th harmonics, is not shared proportionally between DG_1 and DG_2; it is represented in Figures 12(a) and (b).

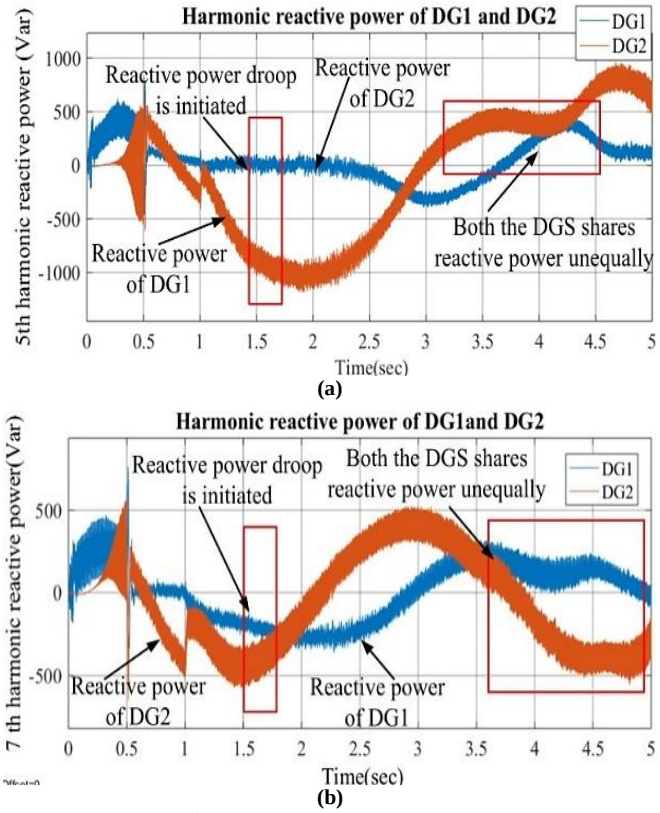

Fig. 12(a) Sharing of the 5th harmonic reactive power among the DGs with non-linear load, and (b) Sharing of the 7th harmonic Reactive power among the DGs with non-linear load.

This harmonic reactive power sharing discrepancy can lead to operational inefficiencies and power quality issues. The simulation results shown in Figures 12 (a) and (b) illustrate that DG_1 and DG_2 fail to equally contribute to the compensation of the 5th and 7th harmonic reactive power, which is crucial for maintaining voltage stability and minimizing harmonic distortion in the system.

5.3. Implementation of ERPDC Method

To address the unbalanced sharing of power between two DGs, the ERPDC concept is implemented in a developed MATLAB model. The obtained wave forms of the 5th and 7th harmonic reactive power waveforms are presented in Figures 13 (a) and (b). For both harmonic conditions, the reactive power droop controller is initiated at around 1.5 sec to 1.7 sec. With the successful implementation of the reactive power droop controller, the system starts its stabilization and shares power equally among the two DGs from 2.5 seconds onwards. The same can be observed in Figures 13 (a) and (b). Thereby, from Figures 13 (a) and (b), it ensures that both DGs contribute equally to the harmonic reactive power, addressing the imbalance that typically occurs when nonlinear loads are present. The equal sharing of harmonic reactive power helps mitigate the potential negative impacts of uneven power distribution, such as voltage instability or excessive harmonic distortion. This balanced sharing not only improves the overall efficiency of the system but also promotes the reliable operation of the grid, with reduced harmonic distortion and improved power quality.

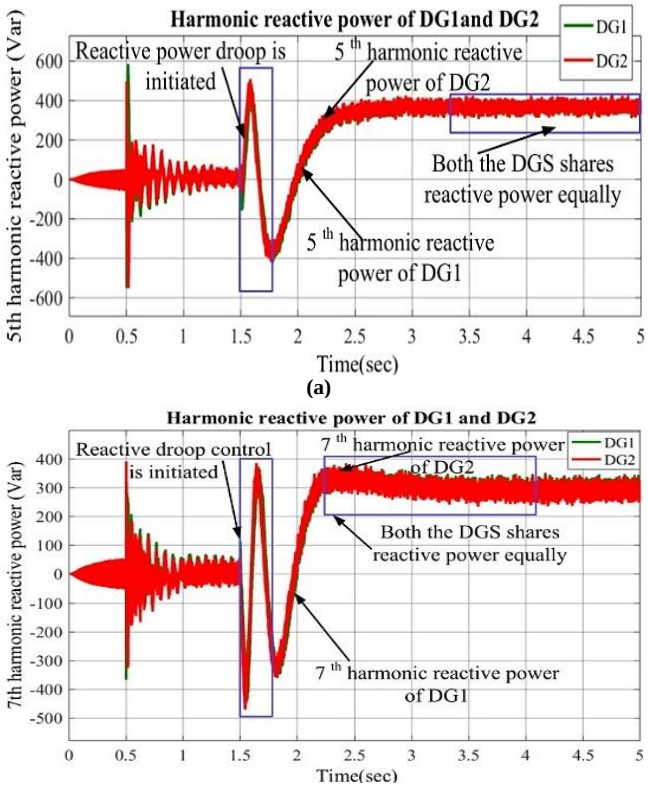

Fig. 13 Waveforms of power (a) Sharing of the 5th harmonic reactive power among the DGs with non-linear load, and (b) Sharing of the 7th harmonic reactive power among the DGs with non-linear load.

5.4. Comparative Analysis and Discussion

In addition to the above results, a comparative analysis for 5th and 7th Harmonic reactive powers using the Modified droop controller and ERPDC methods is presented in Table 2. From Table 2, it can be observed that, for the 5th harmonic reactive power using the modified droop controller, power sharing between two DGs can be observed at 500 and 100 Vars.

Whereas implementing the reactive power droop controller, the power is distributed equally between two DGs, i.e., 400 Vars. Similarly, for the 7th harmonics in the case of implementing the modified droop controller, power sharing between two DGs is -500 and -100 vars.

Table 2. Comparative analysis of harmonic levels

S. No	Parameters	Modified droop controller		Reactive power droop controller	
		DG1	DG2	DG1	DG2
1	5^{th} Harmonic reactive power (Var)	500	100	400	400
2	7^{th} Harmonic reactive power (Var)	-500	-100	360	360

Table 3. Comparison of different controllers

Aspects	Control Type	Stability	Power Sharing Accuracy	Frequency deviation	Voltage Drop Compensation	Impact on Harmonics	Implementation Cost	Communication Requirement	Robustness to Disturbances
Conventional Drop Controller	Primary	Moderate	Moderate	Significant	No	Less	Low	Not required	Low
Improved Conventional Drop Controller	Primary	Enhanced	Improved	Reduced	Partial	Moderate	Moderate	Not required	Moderate
Secondary control strategy	Secondary	Enhanced	Good	Minimal	High	High	High	Required	High
Centralized controller	Secondary	Good	Good	Minimal	High	High	High	Required	Moderate
Decentralized Controller	Primary/ Secondary	Moderate	Improved	Control strategy	Moderate	Moderate	Moderate	Partially Required	Moderate
Adding Virtual inductor/ capacitor	Primary	Enhanced	Improved	Reduced	With virtual impedance	Moderate	Moderate	Not required	High
Robust droop controller	Primary/ Secondary	Good	Good	Very low	High	High	Moderate	Partially Required	High

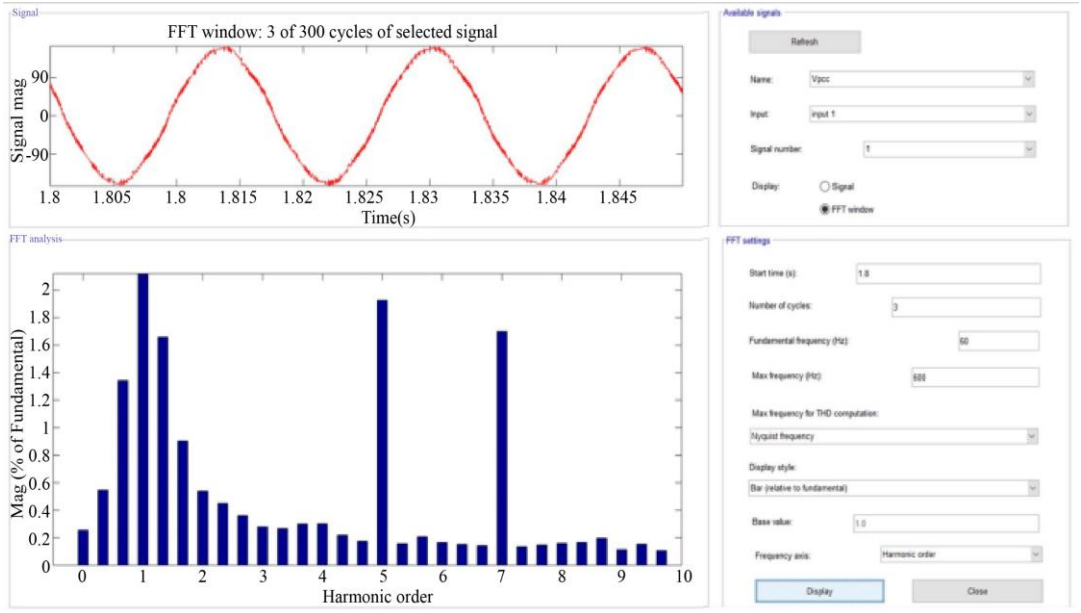

Fig. 14 Total harmonic distortion of the voltage at the point of common coupling

However, implementing the ERPDC method will involve 360 var in both the DGs. In addition, the reduction of circulating currents among parallel-operated inverters leads to an improvement in THD, i.e., 4.84 %. It can be observed in Figure 14. Therefore, from the presented comparative results, it can be confirmed that the ERPDC method works effectively in power sharing among two DGs.

Comparison of different controllers as shown in Table 3. The novelty of this concept is that it enables simultaneous and proportional sharing of both reactive power and harmonic currents. In addition, it integrates harmonic current compensation within the droop control framework and utilizes a modified virtual impedance concept to enhance harmonic sharing. Furthermore, the controller ensures accurate load sharing under nonlinear and unbalanced load conditions, supports plug-and-play capability for Distributed Energy Resources (DERs), and ultimately enhances power quality and system stability in islanded Microgrid operation.

6. Conclusion

This paper used the concept of ERPDC to allocate reactive power among DGs at specific harmonic frequencies for low-voltage islanded Microgrid systems. This controller is based on core principles for delivering power to a constant current source and operates independently of the type of impedance. This controller produces a reference harmonic voltage matching the frequency, reducing the voltage drop across the inverters output impedance. This enables accurate reactive power sharing among the DGs at the correct frequency while ensuring the even distribution of harmonic currents. As a result, the inverter's output voltage stays sinusoidal. The harmonic voltage distortion at PCC significantly reduces the circulation of harmonic currents to a tune of 4.84%, and the harmonic reactive power is shared equally among the DGs. Future research can focus on extending the ERPDC approach to dynamically adapt to varying load conditions and topological changes in real-time. The integration of adaptive machine learning algorithms into the ERPDC framework may further enhance its responsiveness and accuracy in managing harmonics and reactive power sharing. Additionally, exploring the controller's performance under unbalanced load conditions, higher-order harmonics, and during plug-and-play operations of DGs would contribute to the development of more resilient and scalable microgrid control strategies.

References

[1] Saeed Sepasi, Celia Talichet, and Abrar Shahriar Pramanik, "Power Quality in Microgrids: A Critical Review of Fundamentals, Standards, and Case Studies," *IEEE Access*, vol. 11, pp. 108493-108531, 2023. [CrossRef] [Google Scholar] [Publisher Link]

[2] Morteza Hesami, Mirhamed Pourmirasghariyan, and G.B. Gharehpetian, "Microgrids: Characteristics and Emerging Challenges," *2024 11th Iranian Conference on Renewable Energy and Distribution Generation (ICREDG)*, Yazd, Iran, pp. 1-8, 2024. [CrossRef] [Google Scholar] [Publisher Link]

[3] Ilyas Bennia et al., "Stability and Reactive Power Sharing Enhancement in Islanded Microgrid via Small-Signal Modeling and Optimal Virtual Impedance Control," *International Transactions on Electrical Energy Systems*, vol. 2024, pp. 1-25, 2024. [CrossRef] [Google Scholar] [Publisher Link]

[4] Ghazanfar Shahgholian, Mohammadreza Moradian, and Arman Fathollahi, "Droop Control Strategy in Inverter-Based Microgrids: A Brief Review on Analysis and Application in Islanded Mode of Operation," *IET Renewable Power Generation*, vol. 19, no. 1, pp. 1-19, 2025. [CrossRef] [Google Scholar] [Publisher Link]

[5] Tanushree Rai, Anurag Tripathi, and Anurag Verma, "Parallel-Connected Distribution Generation System Operating in Islanded Mode Using Improved Droop Control Technique," *2024 International Conference on Signal Processing and Advance Research in Computing (SPARC)*, LUCKNOW, India, pp. 1-6, 2024. [CrossRef] [Google Scholar] [Publisher Link]

[6] Usman Bashir Tayab, and Qazi Muhammad Humayun, "Enhanced Droop Controller for Operating Parallel-Connected Distributed-Generation Inverters in a Microgrid," *Journal of Renewable and Sustainable Energy*, vol. 10, no. 4, 2018. [CrossRef] [Google Scholar] [Publisher Link]

[7] A. Venkat Rao et al., "Construct and Performance Investigation of a Hybrid ANFIS Controlled Islanded Micro-Grid," *International Journal of Renewable Energy Research*, vol. 15, no. 1, pp. 161-171, 2025. [CrossRef] [Google Scholar] [Publisher Link]

[8] Wei Sun et al., "Secondary Control of Islanded Microgrids with Variable Topology," *2024 IEEE 7th International Electrical and Energy Conference (CIEEC)*, Harbin, China, pp. 4170-4175, 2024. [CrossRef] [Google Scholar] [Publisher Link]

[9] Jingxi Yang, and Chi Kong Tse, "Stability of Islanded Microgrids Considering Distributed Secondary Control," *Complex Behavior of Grid-Connected Power Electronics Systems*, pp. 241-272, 2024. [CrossRef] [Google Scholar] [Publisher Link]

[10] Reda Rabeh, Mohammed Ferfra, and Ahmed Ezbakh, "Secondary Control of Islanded Microgrids Using Cascade PID Controllers Tuned by Combined GA and TLBO Algorithm," *International Journal of Renewable Energy Research (IJRER)*, vol. 13, no. 3, pp. 1297-1310, 2023. [CrossRef] [Google Scholar] [Publisher Link]

[11] Qobad Hafiee, Josep M. Guerrero, and Juan C. Vasquez, "Distributed Secondary Control for Islanded Microgrid-A Novel Approach," *IEEE Transactions on Power Electronics*, vol. 29, no. 2, pp. 1018-1031, 2014. [CrossRef] [Google Scholar] [Publisher Link]

[12] Juan Roberto Lopez et al., "A Decentralized Passive Islanding Detection Method Based on the Variations of Estimated Droop Characteristics," *Energies*, vol. 14, no. 22, pp. 1-19, 2021. [CrossRef] [Google Scholar] [Publisher Link]

[13] Shamsul Aizam Zulkifli et al., "Decentralized Adaptive-Virtual-Impedance-Based Predictive Power for Mismatched Feeders in Islanded Microgrids," *International Journal of Renewable Energy Research*, vol. 12, no. 2, pp. 636-645, 2022. [CrossRef] [Google Scholar] [Publisher Link]

[14] Sunghyok Kim, Songchol Hyon, and Yongil An, "Harmonic Power Sharing Control Using Adaptive Virtual Harmonic Impedance in Islanded Microgrids," *International Journal of Emerging Electric Power Systems*, vol. 25, no. 2, pp. 135-148, 2024. [CrossRef] [Google Scholar] [Publisher Link]

[15] Hui Hwang Goh et al., "Harmonic Virtual Impedance Control in Islanded Microgrids for Harmonic Power Sharing and Harmonic Suppression," *CSEE Journal of Power and Energy Systems*, 2024. [CrossRef] [Google Scholar] [Publisher Link]

[16] Ali Gaeed Seger Al-salloomee, Enrique Romero-Cadaval, and Carlos Roncero-Clemente, "Robust Control Scheme for Optimal Power Sharing and Selective Harmonic Compensation in Islanded Microgrids," *Electronics*, vol. 13, no. 18, pp. 1-25, 2024. [CrossRef] [Google Scholar] [Publisher Link]

[17] Asma Dkhil et al., "Robust Fractional PI Controller Design for Stand-Alone Microgrid Underload Variation: An Optimization-based Approach," *International Journal of Renewable Energy Research*, vol. 13, no. 4, pp. 1526-1537, 2023. [CrossRef] [Google Scholar] [Publisher Link]

[18] Ayman Alhejji et al., "A Robust Cascaded Controller for Load Frequency Control in Renewable Energy Integrated Microgrid Containing PEV," *International Journal of Renewable Energy Research*, vol. 13, no. 1, pp. 435-445, 2023. [CrossRef] [Google Scholar] [Publisher Link]

[19] Nagesh Geddada, and Mahesh Kumar Mishra, "LCL Filters with Active Damping Using PI and SSI Regulators in Synchronous Rotating Reference Frame Current Controller for DSTATCOM," *International Journal of Emerging Electric Power Systems*, vol. 14, no. 4, pp. 309-326, 2013. [CrossRef] [Google Scholar] [Publisher Link]